Available online at www.sciencedirect.com

ScienceDirect

Energy Procedia 129 (2017) 1055–1062

Energy Procedia

www.elsevier.com/locate/procedia

IV International Seminar on ORC Power Systems, ORC2017
13-15 September 2017, Milano, Italy

A revised Tesla Turbine Concept for ORC applications

Giampaolo Manfrida[a]*, Leonardo Pacini[a], Lorenzo Talluri[a]

[a]*Department of Industrial Engineering, University of Florence, Florence, Viale Morgagni 40-44, 50134, Italy*

Abstract

The TESLA turbine is an original expander working on the principle of torque transmission by wall shear stress. The principle – demonstrated for air expanders at lab scale - has some attractive features when applied to ORC expanders: it is suitable for handling limited flow rates (as is the case for machines in the range from 500W to 5 kW), it can be developed to a reasonable size (rotor of 0.1 to 0.3 m diameters), with possible rotational speeds (which range from 1000 to 12000 rpm). The original concept was revisited, improving the stator layout (which is the main responsible for poor performance) and developing a modular design allowing to cover a wide power range, as well as a perfectly sealed operation and other fluid dynamics improvements. The flow model was developed using complete real fluid assumptions, and includes several new concepts such as bladed channels for the stator and detailed treatment of losses. Preliminary design sketches are presented and results discussed and evaluated.

Peer-review under responsibility of the scientific committee of the IV International Seminar on ORC Power Systems.

*Keywords:*Tesla Turbine; Micro-Expander; ORC

1. Introduction

In recent years, energy systems research has been focused on small, distributed systems for cogeneration, which cover the requirements of heat and power generation both in domestic buildings and industrial facilities, with an emphasis on smart grid solutions which can effectively deal with problems of load/generation mismatch and integration of energy storage. When applied to intermediate and low temperature resources, a recurrent technology is the Organic Rankine Cycle, whose applications being extended to small size (5-50 kWe).

* Corresponding author. Tel.:+39 055 2758676; fax: +39 055 2758755.
E-mail address: giampaolo.manfrida@unifi.it

1876-6102
Peer-review under responsibility of the scientific committee of the IV International Seminar on ORC Power Systems.
10.1016/j.egypro.2017.09.115

One of the main problems with micro Organic Rankine Cycles is linked to the expander, as this component often involves high manufacturing costs and offers low reliability. The Tesla turbine, with its relatively simple structure, appears to be a reliable and low-cost expander, which could find its market in the low-power range.

Nomenclature

D_s	Specific diameter [-]
$\dot{m}$	Channel mass flow rate [kg/s]
n_s	Specific speed [-]
0,1,2	Referred to section 0,1,2 (fig. 1b)
h	Enthalpy [kJ/kg]
ORC	Organic Rankine Cycle
p	Pressure [Pa]
r	Radius [m]
u	Peripheral velocity [m/s]
v	Absolute velocity [m/s]
V	Volumetric flow rate [m^3/s]
w	Relative velocity [m/s]
ζ	Loss coefficient [-]
μ	Dynamic viscosity, [kg/(ms)]
ξ	Velocity coefficient
ρ	density, [kg/m^3]
ϕ	Flow coefficient [-]
ψ	Work coefficient [-]
ω	Rotational Speed [rad/s]

1.1. Tesla turbine

The first description of the Tesla turbine, also known as friction turbine, was given in the patent, which was registered by Tesla in 1913 [1].

The Tesla turbine is characterized by a bladeless rotor configuration. Indeed, the rotor is composed of multiple parallel flat disks. The gap between the disks is a fundamental design parameter for this expander. The size of the gap influences the pressure drop produced by friction forces and the exchange of momentum. A very tight gap is required in order to improve work exchange with attractive rotor-only efficiencies (75-90%) [2].

After the pioneer Tesla work, it was only in the 1950s that further study on the bladeless turbine was developed [3]. Another 15 years passed before Rice [4] developed a sound analytic/numerical model of the flow in the Tesla turbine, and performed a full set of experimental investigations.

More recently, several works have been published on the Tesla turbine, both with numerical [5; 6] and experimental contents [7]. Almost all numerical simulations consider the working fluid as incompressible [2; 8]. In experimental tests, the working fluids are generally air or water [7; 9].

Only in very recent times the Tesla turbine has been considered at as a suitable expander for ORC [10; 11].

The main scope of this study is to enrich the mathematical model developed in [12] with a detailed stator model and with non-rotoric components loss correlations; the model (compressible real fluid assumptions) is then applied to organic working fluids in order to assess the performance of the Tesla turbine within this context. A main objective is also to introduce a modular design of the machine so that it can be easily adapted to the specific application.

2. Flow modeling

The Tesla turbine is a viscous turbine, with similar characteristics to drag turbines. The position of the Tesla turbine on the Balje diagram is in the same location of drag turbine and volumetric expanders (very low specific speed, relatively high specific diameter) [13].

Compared to traditional drag turbines and volumetric expanders the main advantage of the Tesla turbine is its relatively simple structure, which results in a low-cost expander. According to simulations, the thermodynamic efficiency of the Tesla turbine appears to be potentially above that of traditional drag turbines and in line with that of volumetric expanders (50-60% when designed for optimal ORC efficiency).

2.1. Stator Flow

As the most original component of a Tesla turbine is the bladeless rotor, simple nozzles are commonly used to generate the necessary highly tangential flow stream at rotor inlet; however, as recognized by [3, 9, 14], the large total pressure loss at stator exit represents a major contribution to the expander inefficiency. Consequently, it was decided to apply to the Tesla turbine stator a design approach derived from radial turbo expanders vaned stator [15, 16, 17], modified with partial admission in order to deal with considerably reduced flow rates. The preliminary sizing of the nozzle starts from the selection of the non-dimensional parameters [15]. Not only fundamental non-dimensional parameters, but also the total thermodynamic conditions at stator inlet represent required inputs (Table 1). Further input geometric parameters are the height and number of stator vanes, which depends on the selected rotor inlet diameter, as well as on the width of the rotor channels.

Table 1. Input parameter for Stator model.

Parameter	Unit	Parameter	Unit
Inlet Total Pressure	[Pa]	Nozzle Throat Mach number	[-]
Inlet Total Temperature	[K]	Specific speed $n_s = \frac{rpm\sqrt{\dot{V}_2}}{60\pi\,\Delta h_{0s}}$	[-]

A relevant feature implemented in the flow model is that the working fluid is treated as a real fluid (that is, neither incompressible nor ideal gas); thermodynamic properties are evaluated locally with real fluid assumption, at present using the Engineering Equation Solver library data[18]. Figure 1 (a) displays the iterative design process as it was implemented in the stator: the output of the process are two loss coefficients, ζ_D and ζ_R, whose values are equaled iteratively until convergence is reached for a given geometry. The first loss coefficient (ζ_D) is expressed in equation 1 as suggested in [15,17] and it is only dependent on ξ, which is the ratio between the real and isentropic velocity at stator exit. The range of this parameter is between 0.9 and 0.97. The second loss coefficient (ζ_R) [17] is on the other hand dependent on geometry values, such as chord, pitch, stator height and stator exit angle, as well as on the Reynolds number of the flow, as displayed in equation 2.

$$\zeta_D = \frac{h_1 - h_{1s}}{\frac{1}{2}v_1^2} = \frac{1}{\xi^2} - 1 \tag{1}$$

$$\zeta_R = \frac{0.05}{Re^{0.2}} * \left(\frac{3\cdot tg\alpha_1}{s/x} + \frac{s\cdot cos\alpha_1}{b_1}\right) \tag{2}$$

Where:

b_1- Blade height at stator outlet [m]; α_1- Absolute angle at stator outlet [°];
s- Blade spacing [m]; x- Chord [m];
Re - Reynolds number (based on blade height and absolute velocity at stator outlet)

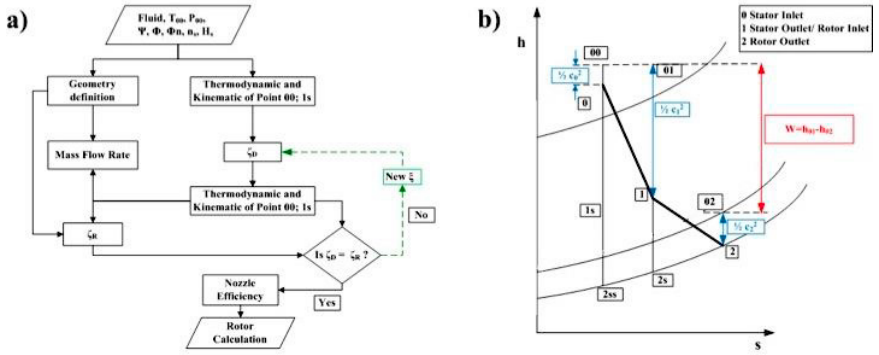

Fig. 1 (a) Flow Diagram of Stator model; (b) Enthalpy-Entropy Diagram of Tesla turbine

2.2. Rotor Flow Model

The model for the rotor flow is derived from [2; 4; 6] with some notable changes; specifically, in line with the stator flow model, the hypothesis of incompressible flow with constant density is removed. Density and viscosity – as well as all other thermodynamic functions – are taken as fluid properties depending on the local variables (typically, p and T), applying a real fluid model. This excludes the possibility of an analytical solution [8].

The complete set of equations applied are reported in [12]; only the main equations of the two-dimensional flow model are here recalled.

Continuity:

$$\frac{1}{r}\frac{\partial(r\rho v_r)}{\partial r} = 0 \tag{3}$$

From momentum, r-direction:

$$\left(\frac{\partial p}{\partial r}\right) = -\frac{12\mu}{b^2}\left(\frac{\dot{m}}{2\pi r b\rho}\right) + \frac{\rho}{r}\left(\frac{\dot{m}}{2\pi r b\rho}\right)^2 + \frac{\rho}{r}{v_\theta}^2 \tag{4}$$

From momentum, θ-direction:

$$\frac{\partial v_\theta}{\partial r} = \frac{24\,\mu\,\pi\,r\,w_\theta}{b\,\dot{m}_c} - \frac{v_\theta}{r} \tag{5}$$

The model was validated with respect to published (incompressible flow) results (figure 2a); the effect of variable density is shown in figure 2b.

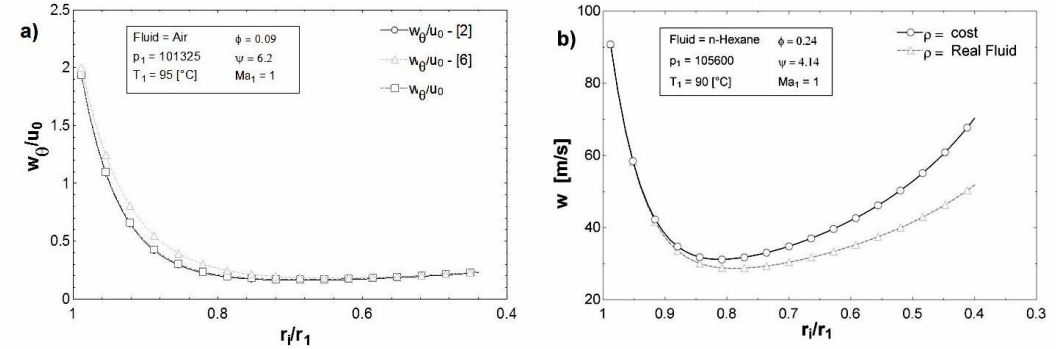

Fig. 2 (a) Validation of model respect to published literature; (b) Variable density influence on relative tangential velocity

2.3. Stator/Rotor coupling Losses

A total pressure loss - accounting for enlargement at stator exit and contraction at rotor inlet, was introduced:

$$\Delta p = \Delta p_e + \Delta p_i = \frac{1}{2}k_e\rho v_1^2 + \frac{1}{2}k_i\rho w_1^2 \tag{6}$$

Where:

Δp_e is the pressure loss which occurs immediately after the throat section(abrupt enlargement);

Δp_i is the pressure loss encountered when the flow enters the rotor micro-channels (relative flow contraction).

The loss coefficient for abrupt enlargement (k_e) is modeled as an incompressible Borda-Carnot coefficient [19] using the velocity immediately before the enlargement. The loss coefficient for contraction (k_i) is obtained through a polynomial fitting of empirical data [19] using the velocity immediately after the contraction.

3. Conceptual Design

In the proposed design, the external carter forms the plenum chamber, which ensures an even flow distribution at a limited number (typically, 4 to 6) of radial nozzle inlets (fig. 3a). The modular design of the machine assembles the stator as a number of stacked disks with machined nozzles, each feeding a larger number of rotor disks (fig. 3b).

The stator compartment is designed to supply the fluid annularly to the rotor. The original shape of the flow channels derives from a one-dimensional design procedure, as described in [15]. After this, partial admission is introduced blocking evenly a number of flow passages in order to realize the required overall flow rate. This evenly applied partial admission solution is a substantial improvement with respect to the common single-nozzle arrangement encountered in lab-scale prototypes of Tesla turbines.

The concept retains some ideas from the original Tesla Patent, which were apparently lost in the following developments. An axial section of the machine is shown in figure 4, showing the possibility of modular adjustment augmenting the axial length and the number of stator/rotor disks; as there is only one shaft exit (although the mechanical design is a sound double-supported shaft), a sealed machine design with magnetic generator couplings also possible, thus allowing the possibility of application with flammable working fluids (hydrocarbons).

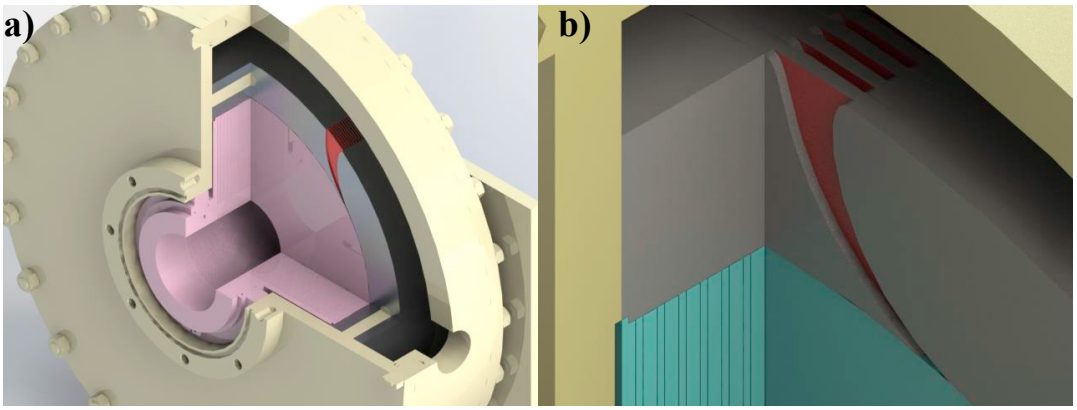

Fig. 3 (a) Tesla turbine, red highlight is the configuration of the plenum chamber; (b) Modularity of the expander

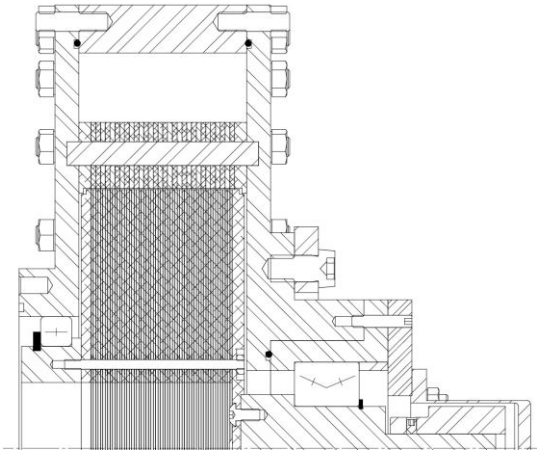

Fig. 4 Tesla turbine axial cross section (hermetic version)

The modularity of the machine allows to cover potentially a wide power range with the same fundamental design, from very small-power applications (the channel power varies between 5-40 W/channel) to a few kWs. In the following, we are referring to the first prototype developed for demonstrating operation on an available test rig operating on a closed-loop with refrigerant fluids; this imposed some restrictions on flow rate, RPM and torque, which are reflected in the final design which is summarized in table 2.

Table 2. Tesla turbine Geometry

Parameter	Section	Unit
Stator inlet diameter	0.25	[m]
Stator outlet/Rotor inlet diameters	0.2	[m]
Effective stator channels	8	[-]
Inlet Stator angle (radial direction)	0	[°]
Outlet Stator angle (radial direction)	85	[°]
Stator Vane Height	0.001	[m]
Rotor outlet diameter	0.08	[m]
Channel Height	0.00012	[m]

4. Working fluid assessment

At the present stage of development, it was important to assess the power and efficiency, which could be reached by the prototype to be tested, depending on working fluid selection. This assessment was carried out on the geometry resumed in Table 2.It is stressed that these constraints limit the actual potential performance: as was shown in [12], the efficiency of the Tesla turbine could reach very high efficiency at the expense of a low power production per channel. At present. the purpose is to demonstrate the concept of the revised Tesla turbine as an ORC expander, and to perform in the future an experimental validation of the flow models.

The fluids here analyzed are R245fa and n-hexane. As low-temperature resource applications are the most likely for this expander, a reference total temperature T_{00} = 100°C was taken as the inlet. The total pressure is different for the two fluids and it was selected in order to have superheated vapor 10°C above saturation temperature (pressure at which the saturation temperature is 90°C).The main parameters evaluated for all simulations are the power per channel, as well as the expander total to static efficiency. The calculations were performed varying the specific speed and the stator outlet Mach number, which was considered a fundamental parameter for the Tesla turbine [9].

4.1. R245fa

As expected, the power of the Tesla turbine increases as the flow coefficient Φ is increased, which is reflected by the nozzle throat Mach number. Higher Mach numbers correspond to large flow coefficients and high mass flow rates. This on one hand increases power, but on the other decreases the total-to-static efficiency.

Another expected feature is the increase in power when Specific Speed n_s is increased. Nonetheless, due to the nature of the machine, the specific speed cannot reach exceedingly high values, due to the increase in the absolute velocity at rotor exit, which after a certain rotational speed would be higher than the value at rotor inlet, with considerable kinetic energy losses at exhaust.

Table 3. Parametric analysis R245fa for Total inlet temperature of 100 [°C] and Inlet Total pressure of 1.009 [MPA]

n_s = 0.001				
Parameter	Ma_1 = 0.4	Ma_1 = 0.6	Ma_1 = 0.8	Ma_1 = 1
Ma_2	0.20	0.40	0.60	0.78
Ψ	5.65	5.69	6.31	7.58
ϕ	0.26	0.31	0.40	0.54
D_s	85.5	77.8	67.9	57.9
RPM	1455	2010	2330	2455
p_2/p_0	0.83	0.63	0.42	0.26
n_s = 0.002				
Ma_2	0.31	0.54	0.75	0.94
Ψ	2.33	2.49	2.92	3.68
ϕ	0.12	0.16	0.21	0.29
D_s	85.2	75.5	64.5	54.2
RPM	3010	3970	4466	4597
p_2/p_0	0.80	0.58	0.38	0.23

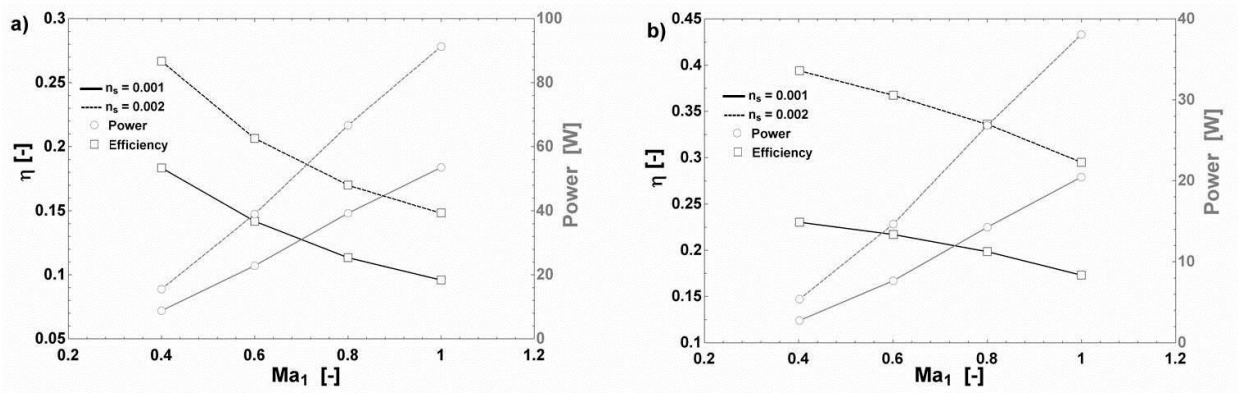

Fig. 5 Efficiency and Power vs. Stator Outlet Mach number for (a) R245fa, (b) n-Hexane

4.2. n-Hexane

Similar results were found for n-Hexane. In particular, the trends for power (increasing with Ma and n_s) and total to static efficiency (increasing with n_s, decreasing with Ma) are the same. However, the values of the total to static efficiency - as well as that of power – were considerably different. Higher efficiencies and lower power production are reached with n-Hexane. This is mainly due to the different inlet pressure of the turbine. Indeed, a total inlet pressure of about 1 MPa was selected for R245fa; on the other hand, the inlet pressure for n-Hexane was much lower (0.18 MPa). Lower pressures mean lower densities; therefore, sonic conditions are reached at the nozzle throat for lower mass flow rates. As shown in [12], low mass flow rates are beneficial for the turbine efficiency, but on the other hand are adverse for power production.

Table 4. Parametric analysis n-Hexane for Total inlet temperature of 100 [°C] and Inlet Total pressure of 0.185 [MPA]

$n_s = 0.001$				
Parameter	$Ma_1 = 0.4$	$Ma_1 = 0.6$	$Ma_1 = 0.8$	$Ma_1 = 1$
Ma_2	0.10	0.16	0.24	0.35
Ψ	6.48	7.02	7.73	8.77
ϕ	0.26	0.30	0.37	0.47
D_s	34.42	32.18	29.44	26.01
RPM	2020	2790	3395	3770
p_2/p_0	0.83	0.66	0.48	0.31
$n_s = 0.002$				
Ma_2	0.16	0.25	0.34	0.46
Ψ	2.81	3.11	3.53	4.14
ϕ	0.12	0.15	0.18	0.24
D_s	34.81	32.05	28.85	25.08
RPM	4285	5795	6885	7475
p_2/p_0	0.81	0.63	0.44	0.28

5. Conclusions

A revised Tesla turbine design was developed in this project and was demonstrated evaluating the performance of two working fluids with a specific prototype size (rotor diameter 0.2 m), referred to the prototype testing on an available test loop. A pivotal point of this research is the conceptual modular design applied for the design of low-power (500W - 5kW) expanders. The key results may be summarised as follows:

- An improved design concept was introduced, tackling stator inefficiency and simplifying the shaft/rotor assembly with a modular, robust construction principle and possibility of sealed operation.
- Due to its intrinsic working principle – work transmitted by friction - the Tesla turbine can be competitive with conventional expanders for low–power application, but it could not become an antagonist for medium to high power as the several losses involved, such as the high kinetic energy at exhaust, increase with the power output per channel. Indeed, the power per channel increases for high inlet Mach number, causing however considerable velocities at discharge and consequently a large kinetic energy loss at exhaust.
- The Tesla turbine rotor performs well with low mass flow rates. Low mass flow rates, for a fixed geometry of the nozzle and fixed velocity at the throat, are obtained for low density at nozzle exit (from continuity equation); therefore, high temperatures and low pressures are necessary for a proper design of the Tesla turbine rotor.
- The results indicate that the Tesla turbine appears potentially competitive with other expanders for low n_s (0.001-0.01) and high D_s (20-80) (typical range for volumetric expanders or drag turbines) with special reference to efficiency. The right range of the flow coefficient for optimum rotor efficiency is very low (Φ = 0.01-0.1). Nonetheless, higher flow coefficients are attractive to increase power output (Φ = 0.05-0.3). On the other hand, the work coefficient Ψ can be very high (over 2). The rotational speed has a strong influence the expander power and efficiency, but generally, the turbine can be sized to work properly within 4000-6000 rpm.

References

[1] Tesla, N., "Turbine", U.S. Patent No. 1 061 206, 1913.

[2] Carey, V.P., "Assessment of Tesla Turbine Performance for Small Scale Rankine Combined Heat and Power Systems", *Journal of Eng. for Gas Turbines and Power*, Vol. 132, 2010.

[3] Armstrong, J.H., "An Investigation of the Performance of a Modified Tesla Turbine", M.S. Thesis, Georgia Institute of Technology, 1952.

[4] Rice, W.; "An analytical and experimental investigation of multiple-disk turbines", *ASME Journal of Engineering for Power*, Vol. 87, Issue 1, pp. 29-36, 1965.

[5] Carey, V.P., "Computational/Theoretical Modeling of Flow Physics and Transport in Disk Rotor Drag Turbine Expanders for Green Energy Conversion Technologies", *Proceedings of theASME 2010 International Mechanical Engineering Congress and Exposition*, Vol. 11, pp. 31-38, 2010.

[6] Guha, A., and Sengupta S., "The fluid dynamics of the rotating flow in a Tesla disc turbine", *European Journal of Mechanics B/Fluids*, Vol. 37, pp. 112-123, 2013.

[7] Hoya, G.P. and Guha, A., "The design of a test rig and study of the performance and efficiency of a Tesla disc turbine", *Proceedings of the Institution of Mechanical Engineers, Part A: Journal of Power and Energy*, Vol. 223, 2009.

[8] Sengupta, S., and Guha, A., "A theory of Tesla disc turbines", *Proceedings of the Institution of Mechanical Engineers, Part A; Journal of Power and Energy*, 2012.

[9] Guha, A., and Smiley, B., "Experiment and analysis for an improved design of the inlet and nozzle in Tesla disc turbines", *Proceedings of the Institution of Mechanical Engineers, Part A: Journal of Power and Energy*, Vol. 224, pp. 261-277, 2009.

[10] Bao, G., Shi, Y., Cai, N., "Numerical modeling research on the boundary layer turbine using organic working fluid", *Proceedings of the International Conference on Power Engineering-13 (ICOPE-13)*, Oct 24-27, Wuhan, China, 2013.

[11] Song, J., Gu, C.W., li, X.S., "Performance estimation of Tesla turbine applied in small scale Organic Rankine Cycle (ORC) system", *Applied Thermal Engineering*, Vol. 110, pp. 318-326, 2017.

[12] Manfrida G., Talluri L., "Fluid Dynamics Assessment of the Tesla Turbine Rotor", *Proceedings of ECOS 2016*, June 19-23, Portoroz, Slovenia, 2016.

[13] Balje, O.E., "Turbomachines, a guide to design, selection and theory", *John Wiley and sons*, New York, 1981.

[14] Neckel A.L., and Godinho, M., "Influence of geometry on the efficiency of convergent-divergent nozzles applied to Tesla turbines", *Experimental Thermal and Fluid Science*, Vol. 62, pp. 131-140, 2015.

[15] Fiaschi, D., Innocenti, I., Manfrida, G., Maraschiello, F., "Design of micro radial turboexpanders for ORC power cycles: From 0D to 3D", *Applied Thermal Engineering*, Vol. 99, 25, pp 402-410, 2016.

[16] Rohlik, H.E., "Radial Inflow Turbines", *NASA SP 290*, Vol. 3, 10, 1975.

[17] Whitfield, A., Baines, N.C., "Design of Radial Turbomachines", *Longman Scientific and Technical*, 1990.

[18] Klein, S.A. and Nellis, G.F., "Mastering EES", *f-Chart software*, 2012.

[19] Idel'chik, I.E., Handbook of hydraulic resistance – coefficients of Local Resistance and of Friction, Springfield: National technical information Service, 1966.